Applied Catalysis B: Environmental 154–155 (2014) 252–258

Contents lists available at ScienceDirect

Applied Catalysis B: Environmental

journal homepage: www.elsevier.com/locate/apcatb

Facile synthesis of sewage sludge-derived mesoporous material as an efficient and stable heterogeneous catalyst for photo-Fenton reaction

Shi-Jie Yuan, Xiao-Hu Dai*

State Key Laboratory of Pollution Control and Resource Reuse, College of Environmental Science and Engineering, Tongji University, Shanghai 200092, China

ARTICLE INFO

Article history:
Received 13 October 2013
Received in revised form 28 January 2014
Accepted 17 February 2014
Available online 24 February 2014

Keywords:
Sewage sludge
Mesoporous material
Heterogeneous photo-Fenton reaction
Visible light irradiation

ABSTRACT

The disposal of sewage sludge, which is produced numerously by wastewater treatment plants worldwide, is currently one of the most important environmental issues. Here we devised an alternative way of converting sewage sludge into mesoporous material (SS-Fe-350) through a facile synthesis method that resulted in an effective and stable heterogeneous catalyst for photo-Fenton reaction. X-ray diffraction, N_2 sorption isotherms and scanning electron microscope analysis indicated the existence of α-Fe_2O_3 within the pores of mesoporous SS-Fe-350 nanocomposite. The original dozens of mg/g of Fe content in the sewage sludge were also collectively identified as the catalytic site. A kinetic analysis showed that SS-Fe-350 exhibited rapid rhodamine B degradation and mineralization under UV light irradiation conditions and *p*-nitrophenol degradation and mineralization under both UV and visible ($\lambda > 400$ nm) light irradiation conditions. The possible reaction mechanism was investigated by the electron spin resonance technique. Moreover, SS-Fe-350 exhibited an excellent stability of catalytic activity and low Fe-ion leaching (<0.7 mg/L). This protocol provides an alternative environmentally friendly sewage sludge reuse method and a facile mesoporous material derived from sewage sludge that effectively degrades azo-dye and refractory organic pollutants.

1. Introduction

Sewage sludge, which consists of organic material, mainly dead bacterial cells, and inorganic component in the form of various oxides and salts, is defined as a pollutant by the US Environmental Protection Agency [1–4]. The annual amount of sewage sludge, which currently comprises about 30 million tons in China [5], 74 million tons in Japan [6], 5.6–7 million dry tons in the US [7] and 9.8 million dry tons in the EU [8], is estimated to increase continuously in the future. Thus, aggravated by their increasing numbers around the world, sewage sludge disposal is perhaps one of the most pressing problems related to water treatment plants currently. Traditional options for sludge disposal such as landfilling and ocean dumping are no longer acceptable, and alternatives such as thermal treatments also raise several concerns [9,10]. Therefore the initiative to reuse of sludge is certainly necessary from an environmental standpoint [11,12].

Heterogeneous photo-Fenton and photo-Fenton-like processes have the unique advantage of being able to completely mineralize organic pollutants by strongly oxidizing hydroxyl radical (OH•) generated, and can easily separate heterogeneous catalysts from treated wastewater while avoiding Fe leaching. They are among the most promising conversion processes for hazardous waste remediation and water disinfection [13–16]. Many studies have been performed and various supports have been used to prepare heterogeneous catalysts for the photo-Fenton process [16–18]. However, many heterogeneous catalysts encounter the leaching problem. The concentration of Fe ions is usually high due to a significant degree of leaching out from the heterogeneous catalysts during the photo-Fenton process, which not only causes the catalysts to lose their activity but also generates secondary metal ion pollution. In such cases, a cost-effective heterogeneous catalyst with high catalytic activity and long-term stability is essential to elevate catalytic efficiency and application.

Fe-based coagulants are among the most widely used coagulants in wastewater treatment plants worldwide, and the amount of Fe content in sewage sludge is significant, comprising dozens of mg/g of dried sludge [3,19,20]. Sewage sludge has been converted into mesoporous adsorbents and used to remove organics in the final stages of water cleaning, absorb acidic gases such as sulfur dioxide and hydrogen sulfide and remove chlorinated organics [11,20]. These are among the most efficient and environmentally friendly ways to use sewage sludge. It is expected that sewage

* Corresponding author. Tel.: +86 21 65986297; fax: +86 21 65983602.
E-mail addresses: ysj@tongji.edu.cn (S.-J. Yuan), daixiaohu@tongji.edu.cn (X.-H. Dai).

http://dx.doi.org/10.1016/j.apcatb.2014.02.031
0926-3373/

sludge-derived material can be used as a heterogeneous catalyst for photo-Fenton reaction and to achieve high catalytic activity and long-term stability.

We developed a facile synthesis of sewage sludge-derived mesoporous material as an effective and stable heterogeneous catalyst for photo-Fenton reaction, and characterized and implemented it for the discoloration and mineralization of azo-dye under UV light irradiation conditions and organic pollutants under both UV and visible ($\lambda > 400$ nm) light irradiation conditions. For our target model pollutants, we chose the widely used Rhodamine B (RhB), which is harmful to humans on contact and toxic to aquatic organisms, and *p*-nitrophenol (*p*-NP), which the US Environmental Protection Agency considers a refractory, hazardous and priority toxic pollutant. We examined the stability of the as-synthesized catalyst and its possible photocatalytic mechanism by the electron spin resonance technique. Our study revealed alternative environmentally friendly ways to dispose of and reuse of sewage sludge, and provided a facile, stable and efficient heterogeneous catalyst for photo-Fenton reaction. To the best of our knowledge, this might be the first attempt of directly converting sewage sludge into a heterogeneous photo-Fenton catalyst under both UV and visible light irradiation conditions.

2. Experimental

2.1. Preparation of the catalysts

The dewatered sewage sludge sample used in this study was obtained from the Anting wastewater treatment plants located in Shanghai, China, which have a design capacity of 150,000 m^3/d [5]. The collected sludge was stored at 4 °C before use. All of the organic and inorganic reagents were of analytical grade unless otherwise stated. All of the solutions were prepared with water from a water purification system (Hitech Instrument Co., Shanghai, China).

The dewatered sewage sludge sample was heated to 350 °C in a muffle furnace in air for 3 h to obtain the catalyst known as SS-350. The sewage sludge-derived Fe-loading mesoporous material was prepared as follows: 10 g of dewatered sewage sludge was added to 20 ml 1 M $FeSO_4 \cdot 7H_2O$ solution and stirred for 3 h at room temperature. The Fe-loading sewage sludge was then recovered via centrifuging and dried in air at 105 °C overnight. Finally, the dried solid, which was designated SS-Fe-105, was calcined in air at 350 °C for 3 h, and the sewage sludge-derived Fe-loading nanocomposite was obtained and designated SS-Fe-350.

2.2. Characterization of the as-synthesized catalysts

Fourier transform infrared (FTIR) spectra were obtained on a KBr disk with a VERTEX 70 FT-IR (Bruker Co., Germany) to determine the functional groups of catalysts. The crystal structure of the as-synthesized catalysts was characterized via X-ray diffraction (XRD; X' Pert PRO, Philips Co., The Netherlands), and its morphology was observed using scanning electron microscopy (SEM; FEI Co., The Netherlands). The bulk chemical compositions of the catalysts were determined via an X-ray fluorescence spectrometer (XRF, PW2402, Philips Co., The Netherlands), and the Fe content was also measured via inductively coupled plasma spectrometry (ICP, Agilent 720ES, USA) after microwave digestion in a Teflon vessel using a mixture of HNO_3 + HCl + HF. The surface area was calculated according to the Brunauer–Emmett–Teller (BET) method.

2.3. Heterogeneous photo-Fenton degradation of RhB and p-NP

Azo-dye RhB and a typical persistent organic pollutant known as *p*-NP were chosen as the model pollutants to evaluate the photocatalytic activity of the as-synthesized catalysts. The photo-Fenton reactions were performed in a quartz glass cylinder measuring 8.5 cm high and 5.5 cm in diameter and filled with 150 ml of RhB (55.5 mg/L) or *p*-NP (65 mg/L) solution with constant magnetic stirring. A 30-W low-pressure mercury lamp was used as the UV light source and fixed next to the cylinder. For the experiments under visible light ($\lambda > 400$ nm) irradiation, an 11-W Philips GENIE cool daylight lamp was used with 2 M $NaNO_2$ acting as a cutoff filter [21]. The reaction temperatures were kept at 25 °C via an air conditioner. Outdoor experiments under solar light irradiation were also carried out.

During the degradation process, 0.05 g of as-synthesized catalyst was dispersed into the reactor, except for the control test in which no catalyst was added. The suspension was stirred in the dark for 30 min to disperse the catalyst, and then the pH of the reaction solution was adjusted to 4.00 for the sake of consistency. After the first sample was taken, the degradation reaction was initiated by adding 1 ml 3% H_2O_2 into the RhB solution or 1 ml 1.2% H_2O_2 into the *p*-NP solution, respectively, except for the control test in which no H_2O_2 was added. At given time intervals during the reaction, solution samples were taken and centrifuged at 4 °C to immediately remove any catalyst particles.

Electron spin resonance (ESR) signals of radicals trapped by 5,5-dimethyl-1-pyrroline N-oxide (DMPO) were recorded at ambient

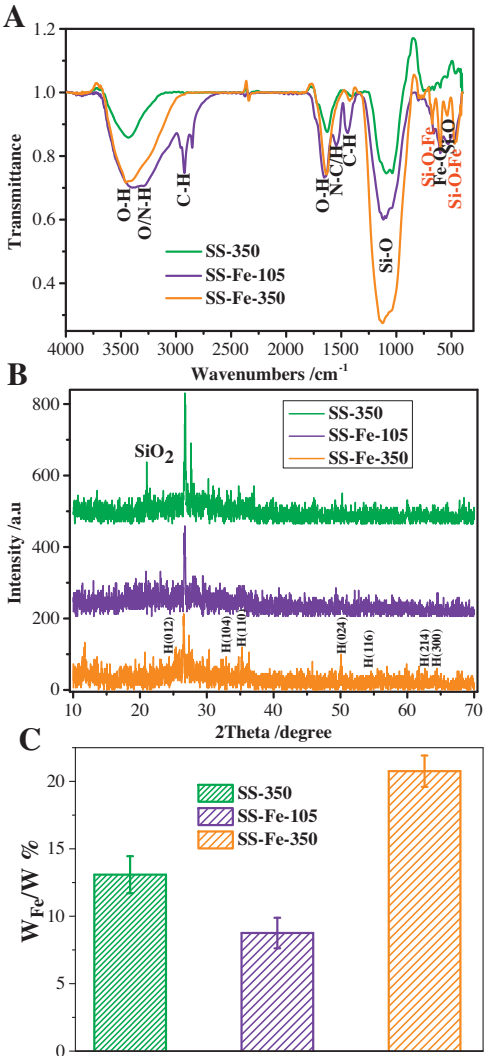

Fig. 1. Characterization of the as-synthesized sewage-sludge-derived catalysts. (A) FTIR spectra. (B) XRD spectrum (H represents hematite). (C) The respective Fe concentration (w/w%).

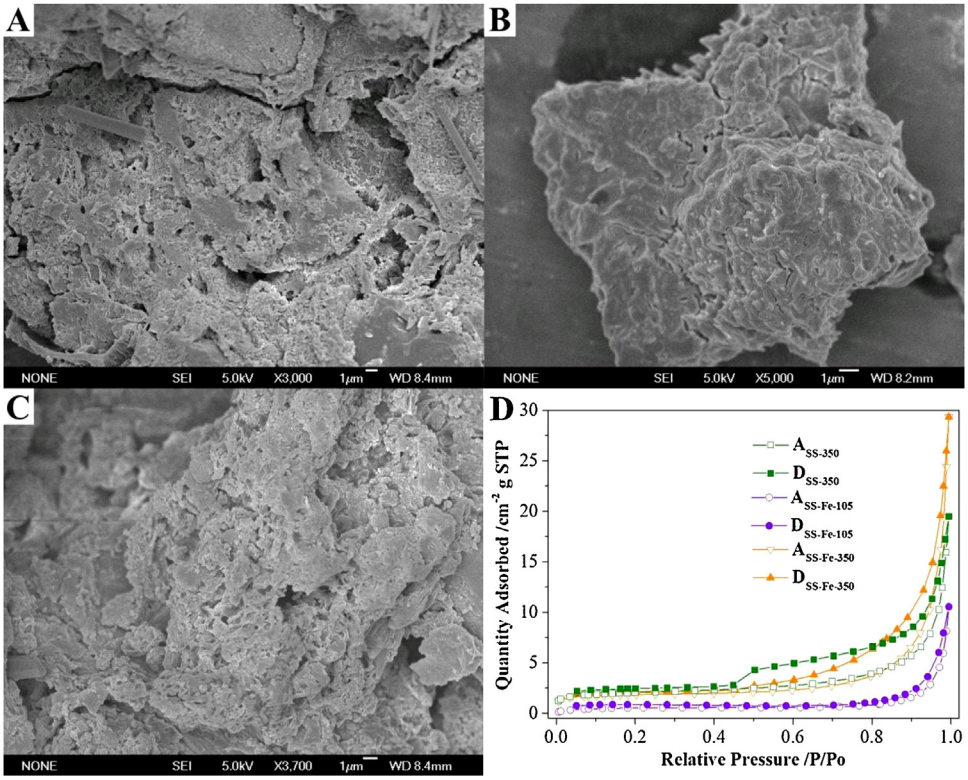

Fig. 2. SEM and N_2 adsorption-desorption isotherms the as-synthesized catalysts. SEM images of (A) SS-350, (B) SS-Fe-105 and (C) SS-Fe-350. (D) N_2 adsorption-desorption isotherms of the as-synthesized catalysts. "A" represents absorption and "D" represents desorption.

temperature on a JEOL JES-FA200 X-band spectrometer (9.072 GHz) (JEOL Co. Japan) with a 500-W Xe-arc lamp as the light source. The concentrations of RhB and *p*-NP were measured during the degradation process via UV–vis spectroscopy (PhotoLab 6100, WTW Co., Germany). The total organic carbon (TOC) concentration was measured using a TOC analyzer (TOC-L CPH CN 200, Shimadzu Co., Japan). The concentrations of Fe and other metal ions in the solution after irradiation were measured via ICP spectrometry to monitor their leaching from the catalysts. All of the tests were conducted in triplicate.

To evaluate the stability and recyclability of the catalyst, SS-Fe-350 was recycled and reused several times to decompose the RhB according to the same conditions under UV and visible light irradiation.

3. Results and discussion

3.1. Characterization of the as-synthesized catalysts

The FTIR spectra were used to determine the functional groups and the chemical bonds on the catalyst surfaces (Fig. 1A). The peaks at 3451 and 1638 cm^{-1} were associated with the O–H stretching vibration and bending vibration, respectively [22]. Comparing curve SS-Fe-105 with curves SS-350 and SS-Fe-350, some peaks were found to disappear, such as the stretching vibration mode of O/N–H (3298 cm^{-1}), the stretching vibration of C–H in the CH_3 and CH_2 groups (2932 and 2852 cm^{-1}), the N–H deformation and C–N stretching vibrations in –CO–NH (1541 cm^{-1}) and the symmetrical deformations of CH_2 (1442 cm^{-1}) [22]. These peak disappearances were mainly attributed to the adsorbed H_2O, small organic molecules and biomacromolecules (e.g., polysaccharide, protein and humic acid) that evaporated, combusted or carbonized during the calcination process. In addition, some new peaks were found in curve SS-Fe-350, such as the characteristic symmetric stretching vibration and bending vibration of the Si–O–Fe (675 and 471 cm^{-1}) [23]. The peak at the 1300–800 cm^{-1} region, which was observed in all three of the curves and enhanced after the Fe loading, was composed of a set of peaks. The broad high intensity band at 1080 cm^{-1} related to the asymmetric Si–O–Si stretching vibrations, the shoulder at 930 cm^{-1} corresponded to a Si–O–Fe linkage and a Si-O-Si symmetrical stretching was assigned at 800 cm^{-1} [24]. These results clearly indicated the formation of chemical bonds between the inorganic compound (SiO_2) in the sewage sludge and the loaded Fe compound in the as-synthesized catalyst SS-Fe-350.

XRD was used to characterize the structure of the as-synthesized catalysts (Fig. 2B). All of the materials displayed two main diffraction peaks at $2\theta = 20.9^\circ$ and 26.7°, which corresponded to typical SiO_2 (quartz) crystallite structures [16]. SS-350 and SS-Fe-350 displayed diffraction peaks at $2\theta = 33.1^\circ$, 35.6° and 50.1°, which were assigned to the (1 0 4), (1 1 0) and (0 2 4) reflections of α-Fe_2O_3 (hematite) (JCPDS, File No. 84-0306). No obvious characteristic

Table 1
Properties of the as-synthesized sewage sludge-derived catalysts.

	SS-350	SS-Fe-105	SS-Fe-350
S_{BET} (m^2/g)	7.16	1.86	6.30
element conc. (wt %)			
Fe	12.9	8.53	19.3
Si	9.72	2.47	6.17
Al	4.29	1.11	2.61
Na	1.25		0.58
Mg	0.82	0.10	0.36
Ca	3.95	0.85	1.71
Ti	0.36	0.12	0.22
Cr	0.17	0.04	0.10
Mn	0.06		0.05
Ni	0.16	0.10	0.13
Cu	0.13	0.04	0.08
Zn	0.46	0.11	0.25

diffraction peak of α-Fe_2O_3 (hematite) was observed in SS-Fe-105, indicating that the α-Fe_2O_3 (hematite) crystallites were formed after calcination at 350 °C. Thus, based on the XRD analysis, we found that SS-350 and SS-Fe-350 mainly consisted of α-Fe_2O_3 (hematite) and SiO_2 (quartz) crystallites, which agreed well with the XRF result (Table 1). The content of Fe in the catalysts was also determined by ICP (Fig. 1C). As the Fe content increased from 13.08 ± 1.38% to 20.76 ± 1.16%, the SiO_2 (quartz) reflections of the samples correspondingly decreased due to the dilution of silica with an increased Fe loading.

SEM and N_2 sorption methods were used to characterize the surface morphology and specific surface areas of the as-synthesized catalysts (Fig. 2 and Table 1). Synthesized by calcination at 350 °C, SS-350 and SS-Fe-350 displayed porous structures that increased the surface areas of the catalysts (Fig. 2A and C and Table 1). These rough structures were more likely attributable to the evaporation, combustion or carbonization of the adsorbed H_2O, small organic molecules and biomacromolecules during the calcination process (Fig. 1A). SS-Fe-105 displayed a relatively solid structure (Fig. 2B). Fig. 2D and Table 1 show the N_2 adsorption–desorption results of the as-synthesized catalysts. According to the IUPAC classification, all of the isotherms were type IV and typical of large-pore mesoporous solids. As revealed by the SEM, SS-Fe-105 displayed a remarkably smaller surface area. The 11.99% reduction of the specific surface areas of the catalysts after Fe loading and calcination probably occurred due to an increase of the material density and the blocking of some pores of the mesoporous material with an increased incorporation of Fe content (α-Fe_2O_3).

The SS-Fe-350 sample, which had chemical bonds between the inorganic compound (SiO_2) and the loaded Fe compound and highest Fe content, provided a large contact area and thus had a high potential to act as a stable and efficient heterogeneous catalyst for the photo-Fenton reaction.

3.2. Photo-Fenton degradation of RhB

Fig. 3A illustrates the UV–vis absorption spectra of the RhB in aqueous solution during the degradation process via H_2O_2 catalyzed with SS-Fe-350 under UV light irradiation conditions. The main absorption band for the RhB was seen at 547 nm, the intensity of which reflected its concentration in the solution. The rapid RhB degradation was clearly evidenced by the change in the peak intensity of the UV–vis absorption spectra, which disappeared absolutely within 20 min. As the absorption spectra in the UV region shifted down remarkably during the degradation process, a high mineralization was expected.

A comparison between the RhB removals versus time under different conditions is shown in Fig. 3B. The linear relationship of $\ln(C_t/C_0)$ versus t shows that the RhB degradation under different photo-Fenton conditions followed the pseudo-first-order kinetics:

$$\ln \frac{C_t}{C_0} = -kt$$

where C_t/C_0 is the normalized RhB concentration, t is the reaction time (min) and k is the reaction rate constant (min^{-1}).

No obvious RhB removal was detected in the reactor without photo-Fenton reaction (i.e., in the presence of UV light or H_2O_2, respectively, but without a catalyst added or with UV light and a catalyst added but without H_2O_2 added). The simultaneous presence of SS-Fe-350 and H_2O_2 or UV light and H_2O_2 resulted in a significant RhB degradation at reaction rate constants of 0.0259 ± 0.0016 min^{-1} and 0.0445 ± 0.0025 min^{-1}, respectively, indicating the catalytic ability of SS-Fe-350 and UV light to activate H_2O_2. The RhB degradation occurred most rapidly in the presence of as-synthesized catalysts and H_2O_2 under UV light irradiation conditions. SS-Fe-350 had the greatest degradation rate constant of 0.282 ± 0.015 min^{-1}, significantly higher than those of SS-350 (0.082 ± 0.006 min^{-1}), SS-Fe-105 (0.176 ± 0.011 min^{-1}) and the commonly used photocatalyst P25 (0.0025 ± 0.0003 min^{-1}) with the same dose under the same conditions. This indicates that the as-synthesized catalysts degraded the azo-dye effectively, and that SS-Fe-350, which had the highest Fe content and larger surface area, exhibited the best catalyst activity.

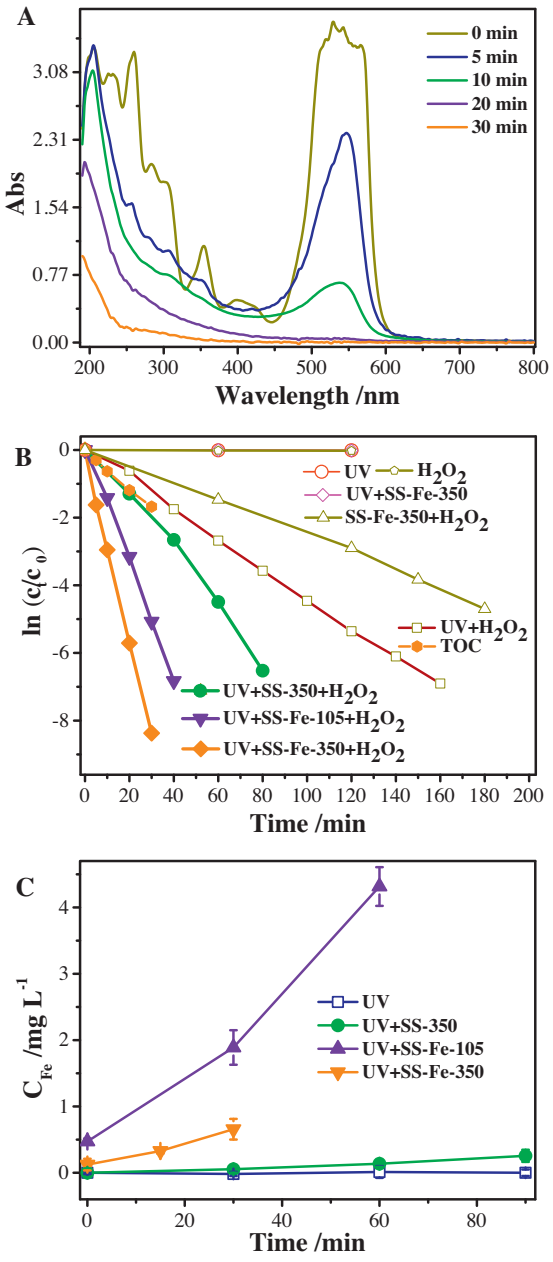

Fig. 3. Catalytic activity and Fe leaching of the as-synthesized catalysts. (A) UV–vis spectra of a typical degradation process under UV light irradiation with both H_2O_2 and SS-Fe-350 added. (B) The relative concentration profiles of RhB and TOC during typical degradation processes under various conditions. (C) Fe concentration in the solution as a function of time (UV: with UV light irradiation but with neither H_2O_2 nor catalyst added; H_2O_2: with H_2O_2 added but with neither UV/visible light irradiation nor catalyst added; UV + catalyst: with both UV light irradiation and catalyst added but without H_2O_2 added; catalyst + H_2O_2: with both H_2O_2 and catalyst added but without UV light irradiation; UV + H_2O_2: with both UV light irradiation and H_2O_2 added but without any catalyst added; and UV + catalyst + H_2O_2: with UV light irradiation and both H_2O_2 and catalyst added).

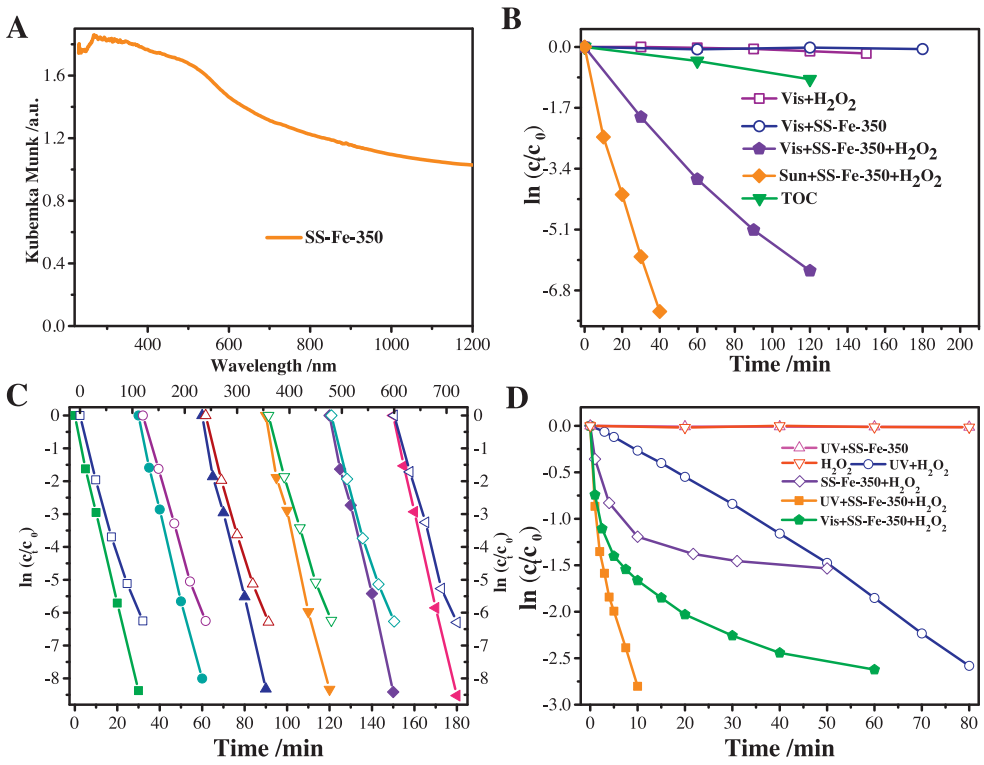

Fig. 4. Diffuse reflectance UV–vis spectra and catalytic activity of SS-Fe-350 under visible irradiation conditions. (A) Diffuse reflectance UV–vis spectra of SS-Fe-350. (B) Relative concentration profiles of RhB and TOC during typical degradation processes under various visible light irradiation conditions. (C) Cyclic degradation in repetitive degradation of RhB under UV (closed symbols) and visible (open symbols) light irradiation conditions. (D) Relative concentration profiles of *p*-NP during typical degradation processes under various conditions. The legends are similar to those of Fig. 3.

The rapid RhB degradation via H_2O_2 catalyzed with SS-Fe-350 was accompanied by a mineralization process. As confirmed by the TOC measurement, with SS-Fe-350 (0.05 g) and H_2O_2 (1 ml 3%) under UV light irradiation conditions, more than 81% TOC of 55.5 g/L RhB was removed after 30 min as expected, suggesting that the SS-Fe-350 catalyst showed a significant degree of RhB mineralization.

The Fe ion concentration in the solution versus the irradiation time of the degradation process was determined via ICP to identify whether the catalysts' heterogeneous photo-Fenton reaction or Fe leaching caused the observed catalytic activity (Fig. 3C). It is clear that the synthetic methods of the catalysts significantly influenced the Fe-ion concentration in the solution. SS-Fe-105 exhibited the highest Fe-ion leaching rate during the degradation process, and its concentration in the solution reached 4.32 ± 0.29 mg/L after 60 min of reaction time. There were barely any Fe ions detected in the control without a catalyst added. For SS-350, the Fe-ion concentrations were slowly increased to 0.26 ± 0.09 mg/L after 120 min of reaction time. A similar result was observed under the SS-Fe-350 conditions (0.66 ± 0.15 mg/L after 30 min), accounting for the formation of chemical bonds between the inorganic material (SiO_2) and the loaded Fe compound. Additional experiment, the degradation of RhB in the presence of 0.66 mg/L Fe^{2+} in solution under the same condition, was conducted. Compared with the control conditions without Fe^{2+} present, a little larger degradation rate constant of $0.0491 \pm 0.0029\ min^{-1}$ was obtain, which was much smaller than the conditions with the present of catalyst. Thus it can be deduced that, when the SS-Fe-350 were used as the catalyst, both heterogeneous and homogeneous photo-Fenton reactions were responsible for the fast degradation of RhB. However, instead of the Fe ions in solution, the main contribution was from the as-synthesized catalyst. This means that the heterogeneous photo-Fenton reaction was mainly responsible for the fast degradation and mineralization of RhB during the photo-Fenton reaction of the SS-Fe-350 catalyst. Other metal ion leaching was rarely detected during any of the reactions with or without catalysts added.

3.3. *Visible photo-Fenton reaction*

The diffuse reflectance UV–vis absorption of SS-Fe-350, which exhibited the best catalyst activity UV light irradiation conditions, was measured to investigate its optical response to visible light irradiation (Fig. 4A). Strong absorption ranging from 400 to 1200 nm was observed, perhaps due to the charge transfer of small inorganic molecules or other metal oxides in the sewage sludge [20]. This made it possible to use SS-Fe-350 as a visible light photoactive catalyst in the photo-Fenton reaction.

RhB and *p*-NP degradation tests were conducted under visible ($\lambda > 400$ nm) light irradiation conditions to confirm the catalytic activity of SS-Fe-350. In the presence of SS-Fe-350 under visible light irradiation conditions but without H_2O_2 added, only slight and inconspicuous RhB degradation was detected. The self-exciting and degradation of RhB was observable in the presence of H_2O_2 under visible light irradiation conditions without any SS-Fe-350 added [25,26], showing a reaction rate constant of $0.000789 \pm 0.0000319\ min^{-1}$. The simultaneous presence of SS-Fe-350 and H_2O_2 under visible light irradiation conditions resulted in a quite significant degradation of RhB with a reaction rate constant of $0.0522 \pm 0.0032\ min^{-1}$, indicating the importance of visible light irradiation to the degradation. More than 59% TOC was removed after 120 min of reaction time, suggesting that SS-Fe-350 also showed a significant degree of RhB mineralization under visible light irradiation conditions. A high reaction rate constant of $0.181 \pm 0.010\ min^{-1}$ was observed under solar illumination conditions due to the presence of both UV and visible light in sunshine (Fig. 4B). The durability of SS-Fe-350 under both UV and visible light irradiation conditions was also measured for practical applications

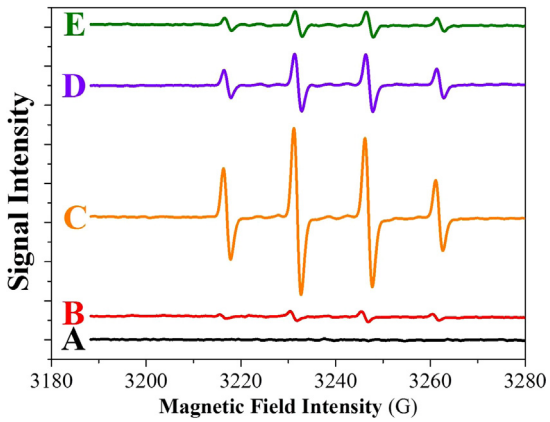

Fig. 5. DMPO spin-trapping ESR spectra of aqueous solution (pH = 4) in the presence of catalyst SS-Fe-350 without UV and visible light irradiation (A), with both UV and visible light irradiation after 60 s (B), with both UV and visible light irradiation and H_2O_2 added after 60 s (C), with UV light irradiation and H_2O_2 added after 60 s (D), and with visible light irradiation and H_2O_2 added after 60 s (E).

(Fig. 4C). No obvious deactivation of the SS-Fe-350 catalyst in the six repetitive experiments was observed when compared with the first cycle, indicating its excellent long-term stability. In view of the negligible Fe leaching from the SS-Fe-350 catalyst during the catalytic reaction, the excellent stability of the catalytic activity could be attributed to the catalyst's stable structure.

Considering that the RhB can act as a photosensitizer under visible light irradiation conditions [25,26], *p*-NP was also used as another target pollutant in this study, especially under visible light irradiation conditions. After 60 min of degradation under visible light irradiation conditions (Fig. 4D), the absorbance and TOC removal rates of the *p*-NP reached 92.74% and 47.25%, respectively, indicating that SS-Fe-350 was also efficient at *p*-NP degradation and mineralization.

3.4. Possible reaction mechanism

ESR was used to detect the generation of OH• under various conditions. While no signal of DMPO-OH• adducts characterized by intensity ratio of 1:2:2:1 could be observed in the presence of catalyst SS-Fe-350 only (A), it became slight and inconspicuous upon light irradiation (B) and evidently increased with H_2O_2 added (Fig. 5), which was in consist with the observed degradation rates of RhB and *p*-NP respectively. No obviously signal of sextet peaks of DMPO-•OOH/O_2•$^-$ adducts were observed under all these conditions, suggested that OH•, other than •OOH/O_2•$^-$, radicals were the mainly active species involved in the H_2O_2 decomposition in the presence of SS-Fe-350 under various conditions (1).

The intensity of DMPO-OH• signal further decreased in the absence of visible light irradiation (C, D), suggested that the electron can transfer from some specific small inorganic molecular or other metal oxides in the sewage sludge, which can be excited by visible light, to the Fe(III) on the as-synthesized catalyst (2) and (3) and initiate degradation and mineralization of target pollutions subsequently only under visible light irradiation conditions (Fig. 6). Compared with the visible light irradiation system (E), a distinctly higher intensity of DMPO-OH• signal was observed in the UV light irradiation system (D), explaining that H_2O_2 decomposition and OH• generation under visible light irradiation conditions was relatively slow, which was in consist with the observed degradation rates of RhB and *p*-NP under these conditions.

$$\mathrm{Fe(II) + H_2O_2 \rightarrow Fe(III) + OH^- + OH\bullet} \quad (1)$$

$$\mathrm{M + h\upsilon \rightarrow M^*} \quad (2)$$

$$\mathrm{M^* + Fe(III) \rightarrow Fe(II) + M\bullet^+} \quad (3)$$

(M here represent for those specific small inorganic molecular or other metal oxides in the sewage sludge, which can be excited by visible light, and RhB.)

With RhB, which could be excited by visible light irradiation [25,26], as the target pollutant, it can also transfer electron to the Fe(III) on the as-synthesized catalyst, assist H_2O_2 decomposition and OH• generation, and initiate degradation and mineralization of itself subsequently under visible light irradiation conditions with a reaction rate constant of $0.000789 \pm 0.0000319\ \mathrm{min^{-1}}$ (Fig. 4B), whereas this self-exciting and degradation process cannot occur under UV light irradiation conditions.

3.5. Significance in application

SS-Fe-350, the efficient and stable heterogeneous photo-Fenton catalyst of a mesoporous material derived from sewage sludge, was synthesized via a facile method (Fig. 6). The facile synthesis method had only three steps and led to savings on operational costs and less investment for equipment. The bacterium, inorganic particles and small inorganic molecules in the sewage sludge were used as scaffold templates for the preparation of the mesoporous material. The mesoporous quality of the catalyst was attributed to the evaporation, combustion or carbonization of the adsorbed H_2O, small

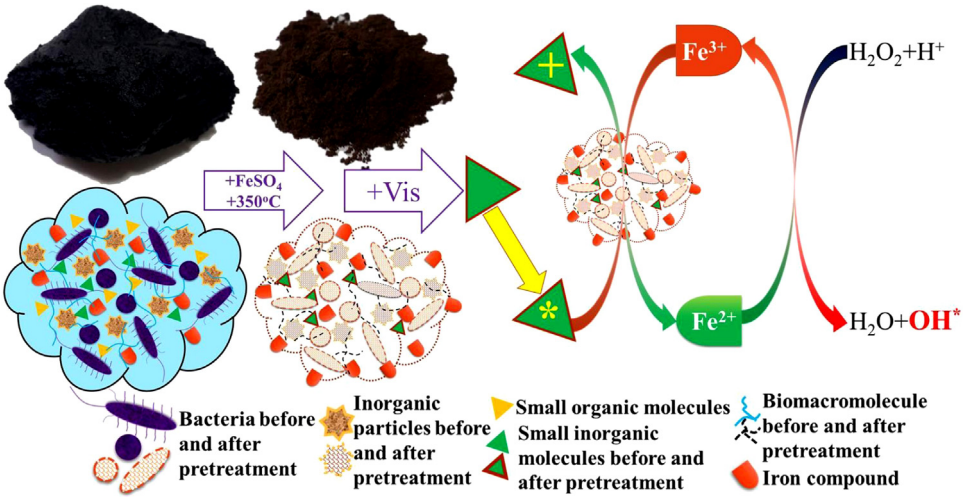

Fig. 6. Schematic diagram of the prepared catalyst SS-Fe-350 and the mechanism of the photo-Fenton reaction under visible light irradiation conditions.

organic molecules and biomacromolecules in the sewage sludge during the calcination process. The original dozens of mg/g of Fe content in the sewage sludge were also collectively identified as the catalytic site. All those type of chemicals which were the usually composed of sewage sludge [1–7], were properly provided for the synthesis of this efficient and stable catalyst (Fig. 6). Thus the sewage sludge we used and its derived catalyst in this research could be taken as a representative materials.

The chemical bonds between the loaded Fe compound and the scaffold templates of the synthesized mesoporous material derived from sewage sludge ensured the absence of Fe leaching during the heterogeneous photo-Fenton reaction and the stability of the catalysts for reuse. The nanocomposite catalyst could be separated easily from the reaction solution via a simple precipitation procedure, as its density increased with the Fe loading. The natural pH of the reaction solution after the addition of 0.05 g/150 ml SS-Fe-350 was 3.4–3.5, for which a more rapid degradation and mineralization rate was expected.

The sludge source and property, especially the Fe content, do have important influence on this preparation. Thus dewatered sewage sludge from industrial wastewater treatment plant or wastewater treatment plant that utilized Fe-based coagulants was more appreciated. The surface area of the as-synthesized catalyst was relatively small compared with the other reported catalysts and sewage sludge-derived adsorbent materials. Several methods such as carbonization, chemical activation, and pyrolysis [11] were expected to increase the surface area. However, these pretreatment methods would accompanied by an unavoidable cost increase and more investment for equipment, thus may not acceptable for practical application and from an environmental standpoint. Despite of the facile synthesis method, the catalyst still relies on multiple-step preparations. During this facile synthesize approach, stir, centrifuge, drying and calcination were carried out successively. Stirrer, centrifuge, oven and muffle furnace were all needed. Also part of the organic matter in the sewage sludge, which was evaporation, combustion or carbonization during this approach, could be converted into biogas alternatively by anaerobic digestion in advance [5], which might be a more thorough and environmentally friendly sewage sludge reuse approach and we will be investigated it in our following work.

After the Fe loading process, some specific small inorganic molecular or other metal oxides in the sewage sludge (Table 1), which were excited by visible light (Fig. 4A), were partially covered by or made contact with the Fe compound. Under visible light irradiation conditions, the excited specific small inorganic molecules and other metal oxides on the surface of SS-Fe-350 would interact with the loaded Fe compound, generate Fe(II) via one-electron transfer and initiate subsequent degradation and mineralization under visible light irradiation conditions (Fig. 6) (2) and (3). The reactions under these conditions supported the inference and suggested the efficient use of rich and natural solar energy to drive the heterogeneous photo-Fenton reaction.

4. Conclusions

In summary, we synthesized a sewage sludge-derived mesoporous material, SS-Fe-350, via a facile three-step method and demonstrated its efficiency and stability as a heterogeneous catalyst for photo-Fenton reaction under both UV and visible irradiation conditions. A kinetic analysis showed that the as-synthesized catalyst exhibited RhB degradation at a rate more than six times the rates of the control reaction without any catalyst added. The leaching of Fe and other metal ions during the heterogeneous photo-Fenton reaction was avoidable. OH•, other than $\bullet OOH/O_2\bullet^-$, radicals were the mainly active species involved in the H_2O_2 decomposition in the presence of SS-Fe-350 under various conditions. The results presented in this paper offer new opportunities for the environmentally friendly reuse of sewage sludge and provide a facile method for synthesizing mesoporous material derived from sewage sludge for the effective degradation of azo-dye and refractory organic pollutants.

Acknowledgements

The authors wish to thank the NSFC (51308401), the National Key Technologies R&D Program of China (2010BAC67B04), the key projects of National Water Pollution Control and Management of China (2011ZX07316-004) and the China Postdoctoral Science Foundation (2013M530209) for their partial support of this study.

References

[1] E. Viau, K. Bibby, T. Paez-Rubio, J. Peccia, Environ. Sci. Technol. 45 (2011) 5459–5469.
[2] M.A. Shannon, P.W. Bohn, M. Elimelech, J.G. Georgiadis, B.J. Mariñas, A.M. Mayes, Nature 452 (2008) 301–310.
[3] G. Ahlberg, O. Gustafsson, P. Wedel, Environ. Pollut. 144 (2006) 545–553.
[4] U.S. Environmental Protection Agency, 1994.
[5] N.N. Duan, B. Dong, B. Wu, X.H. Dai, Bioresour. Technol. 104 (2012) 150–156.
[6] M. Matsubara, T. Itoh, Saisei to riyo (Assoc. Utilizat. Sewage Sludge) 29 (2006) 19–27.
[7] K. McClellan, R.U. Halden, Water Res. 44 (2010) 658–668.
[8] A. Kelessidis, A.S. Stasinakis, Waste Manag. 32 (2012) 1186–1195.
[9] R. Iranpour, M. Stenstrom, G. Tchobanoglous, D. Miller, J. Wright, M. Vossoughi, Science 285 (1999) 706–711.
[10] J.C. Bourgeois, M.E. Walsh, G.A. Gagnon, Water Res. 38 (2004) 1173–1182.
[11] A. Ros, M.A. Montes-Morán, E. Fuente, D.M. Nevskaia, M.J. Martin, Environ. Sci. Technol. 40 (2006) 302–309.
[12] G.R. Xu, J.L. Zou, G.B. Li, Environ. Sci. Technol. 42 (2008) 7417–7423.
[13] J.H. Deng, J.Y. Jiang, Y.Y. Zhang, X.P. Lin, C.M. Du, Y. Xiong, Appl. Catal., B 84 (2008) 468–473.
[14] J.H. Ma, W.J. Song, C.C. Chen, W.H. Ma, J.C. Zhao, Y.L. Tang, Environ. Sci. Technol. 29 (2005) 5810–5815.
[15] A.L.-T. Pham, C.H. Lee, F.M. Doyle, D.L. Sedlak, Environ. Sci. Technol. 43 (2009) 8930–8935.
[16] J.Y. Feng, X.J. Hu, P.L. Yue, Environ. Sci. Technol. 38 (2004) 269–275.
[17] G. Ersöz, Appl. Catal., B 147 (2013) 353–358.
[18] M.B. Kasiri, H. Aleboyeh, A. Aleboyeh, Appl. Catal., B 84 (2008) 9–15.
[19] G. Tchobanoglous, F.L. Burton, H.D. Stensel, Wastewater Engineering, Treatment and Reuse, McGraw-Hill Higher Education, Metcalf & Eddy, Inc., New York, 2003.
[20] K.M. Smith, G.D. Fowler, S. Pullket, N.J.D. Graham, Water Res. 43 (2009) 2569–2594.
[21] T. Ohno, L. Bai, T. Hisatomi, K. Maeda, K. Domen, J. Am. Chem. Soc. 134 (2012) 8254–8259.
[22] J. Schmitt, H.C. Flemming, Biodeterior. Biodegrad. 41 (1998) 1–11.
[23] I. Moriguchi, M. Honda, T. Ohkubo, Y. Mawatari, Y. Teraoka, Catal. Today 90 (2004) 297–303.
[24] E. Doelsch, A. Masion, J. Rose, W.E.E. Stone, J.Y. Bottero, P.M. Bertsch, Colloids Surf., A 217 (2003) 121–128.
[25] M.M. Cheng, W.J. Song, W.H. Ma, C.C. Chen, J.C. Zhao, J. Lin, H.Y. Zhu, Appl. Catal., B 77 (2008) 355–363.
[26] W.J. Song, M.M. Cheng, J.H. Ma, W.H. Ma, C.C. Chen, J.C. Zhao, Environ. Sci. Technol. 40 (2006) 4782–4787.